INVESTIGATION OF COMPUTATIONAL DETERMINATION OF ELASTIC PROPERTIES FOR SILICON NITRIDE AND SILICON CARBONITRIDE MATERIALS

by

TIMOTHY AARON WEST

THESIS
Submitted in partial fulfillment of the requirements
for the degree of Master of Science in Chemistry at
The University of Texas at Arlington
August, 2020

Arlington, Texas

Supervising Committee:
Peter Kroll, Supervising Professor
Kwangho Nam
Krishnan Rajeshwar
Frederick Macdonnell

ABSTRACT

INVESTIGATION OF COMPUTATIONAL DETERMINATION

OF ELASTIC PROPERTIES FOR SILICON NITRIDE

AND SILICON CARBONITRIDE MATERIALS

Timothy Aaron West, Master of Science in Chemistry

The University of Texas at Arlington, 2020

Supervising Professor: Peter Kroll

Silicon nitride and silicon carbonitride materials are versatile materials exhibiting useful properties at high temperatures and pressures. This study investigates the use of molecular dynamics simulations to determine the elastic properties of these materials. Elastic constants and moduli are determined for a series of crystalline and amorphous silicon nitride materials and amorphous silicon carbonitride materials employing Tersoff, Garofalini, and Marian-Gastreich two-body empirical potentials. Our results show that the Tersoff empirical potential is best suited of the three under study to elastic property determination. Results also show that the elastic behavior of silicon carbonitride is highly dependent on the morphology of carbon in the material. This study shows that there is a need for an empirical potential which accurately captures the elastic behavior of these materials at high temperature.

TABLE OF CONTENTS

ABSTRACT…… ii

CHAPTER ONE: INTRODUCTION…….. 1

CHAPTER TWO: METHOD…….. 5

CHAPTER THREE: RESULTS AND DISCUSSION…….. 12

CHAPTER FOUR: CONCLUSION…….. 36

REFERENCES…….. 39

1. Introduction

Polymer-derived silicon carbonitride (SiCN) ceramics are materials exhibiting useful high-temperature mechanical properties. Nanoscale silicon nitride structures have shown promise for use in optoelectronic devices [1], sensors [2], orthopedic implants [3], and drug delivery [4]. Bulk SiCN exhibits oxidation and creep resistance, with a glass transition temperature far higher than that of oxidic glasses such as quartz [5,6,7].

SiCN materials have been prepared by various experimental methods. Thin-film SiCN has been experimentally prepared by chemical vapor deposition (CVD) methods including plasma-enhanced CVD (PECVD) [8,9] and thermal CVD [10], as well as arc-enhanced magnetic sputtering (AEMS) [11]. SiCN films prepared by PECVD have generally consisted of hydrogenated silicon carbonitride, and depending on specific approach, oxygen contents from >0.2% up to 10% have been reported. The resulting films have thicknesses on the order of 400-900 nm, with reported densities in the range of 1.65 – 1.86 g/cm^3, increasing in density with greater content of incorporated oxygen. Reported Young's elastic moduli for these materials is in the range of 110 – 150 GPa [8,9], with higher values of elastic moduli associated with lower working pressures during deposition. SiCN films prepared by thermal CVD report thicknesses an order of magnitude larger than seen with PECVD, ranging from 4.5 – 5.1 um, and reported Young's moduli for these materials range from 165 – 300 GPa [10], increasing with increasing H_2 flow rate during deposition. SiCN films prepared by AEMS report similar thicknesses and mechanical properties to those observed in films prepared with thermal CVD [11].

Furthermore, SiCN bulk ceramic materials have been prepared by cross-linking and pyrolysis of precursor polymers [12], as well as by hot-press sintering [13]. Bulk materials prepared by crosslinking and pyrolysis are reported to contain hydrogen between 2% and 28%, with hydrogen content decreasing as a function of increasing pyrolysis temperature across a range of 800 – 1200 °C, as well as ~2% oxygen content without regard to pyrolysis temperature [12]. These materials report densities in the range of 1.85 – 2.15 g/cm^3 and Young's moduli in the range of 80 – 140 GPa, with both values increasing as a function of increasing pyrolysis temperature. Bulk materials prepared by hot-press sintering at temperatures from 1400 – 1500 °C incorporate a larger amount of oxygen content at 10-15 at.%, and exhibit significant porosity. Consequently, these materials are reported to have significantly lower densities ranging from 1.2 – 1.7 g/cm^3 as well as significantly lower Young's moduli ranging from 14 – 38 GPa [13].

SiCN materials and their mechanical properties have previously been studied through computational methods. Tersoff potential parameters for SiCN were developed and fitted to the lattice parameters, cohesive energy, and bulk moduli of silicon nitride and carbon nitride [14]. The structures and mechanical properties of high-pressure crystalline SiCN phases have been studied using density functional theory [15]. These calculations indicated bulk moduli ranging from 230 – 250 GPa and shear moduli ranging from 160 – 210 GPa depending on the particular high-pressure crystalline phase. In addition, molecular dynamics investigations of mechanical properties utilizing the Tersoff empirical potential have been conducted on bulk Si_3N_4-SiC composites with a 1:1 ratio between Si_3N_4 and SiC [16] as well as

on models including “excess” or “free” carbon [17]. These studies have reported Young’s moduli in the range of 180 – 260 GPa for models without excess carbon with modulus values decreasing with increasing annealing temperature during model generation [16, 17]. With regard to excess carbon, values of Young’s moduli were reported to increase with increasing carbon content [17]. In contrast, a study of amorphous thin-film SiCN materials using density-functional molecular dynamics simulations [18] reported a contradictory trend, with Young’s modulus decreasing as a function of increasing carbon content.

Previously, a comparative study of empirical potentials for simulations of amorphous silicon nitride has been performed [19]. This study compared several empirical interatomic potentials including the Tersoff potential, the Marian-Gastreich two-body (MG2) and three-body (MG3) potentials, the Vashista potential, and the Garafolini potential (SG). This study suggested that the MG2 and SG potentials were the best options for modeling this material. These potentials are employed in the current study of SiCN materials.

In this study, we investigate determination of elastic properties of crystalline and amorphous silicon nitride (Si_3N_4) and amorphous SiCN using molecular dynamics simulations employing Tersoff, Garofalini (SG), and Marian-Gastreich two-body (MG2) empirical potentials. We first investigate Si_3N_4 as a means of validating the computational approach.

Amorphous SiCN is modeled as a stoichiometric mixture of Si_3N_4:SiC, as well as with “excess” or “free” carbon included. This free carbon is of interest due to the formation of large ordered domains of carbon segregation which appear to form in

the SiCN bulk. In our models, these domains consist of sheet-like structures of carbon arranged into six-membered rings resembling graphene.

2. Method

Molecular dynamics simulations are performed as implemented in the Large-scale Atomic/Molecular Massively Parallel Simulator (LAMMPS). All simulations employ the Langevin thermostat and the velocity-Verlet time integrator with a 1 fs time step For Si_3N_4 models, interactions are described using two parametrizations of the Tersoff potential, labeled 001 and BM, and one parametrization each of the SG and MG2 potentials. For SiCN models, only the two parametrizations of the Tersoff potential are used.

2.1. Si_3N_4 Model Generation

Crystalline models of Si_3N_4 were generated by creation of ortho-hexagonal unit cells from hexagonal unit cells described in crystallographic information files (.cif) obtained from the International Crystal Structure Database [20]. From these ortho-hexagonal unit cells, super-cell models were generated to produce a roughly cubic model overall. For alpha-Si_3N_4, conversion of the original hexagonal unit cell to an ortho-hexagonal cell resulted in a model with lattice parameters a = 7.75 Å, b = 13.43 Å, and c = 5.62 Å. A 7×4×10 super-cell was then generated to obtain a model with lattice parameters a = 54.3 Å, b = 53. 7 Å, and c = 56.2 Å. For beta-Si_3N_4, conversion to an ortho-hexagonal cell resulted in a model with lattice parameters a = 7.64 Å, b = 13.23 Å, and c = 2.92 Å. A 7×4×20 super-cell was then generated to obtain a model with lattice parameters a = 53.5 Å, b = 52.9 Å, and c = 58.4 Å. Both super-cell models contain 15,680 atoms and have a density of 3.2 g/cm^3.

a)

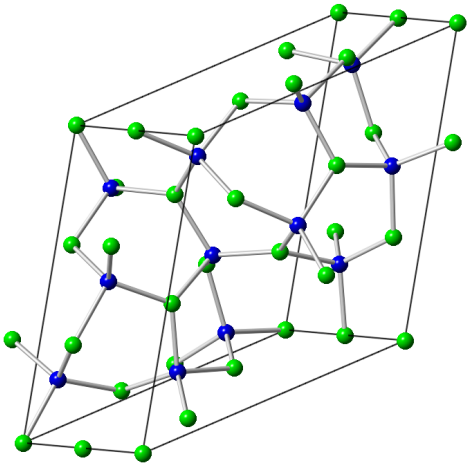

b)

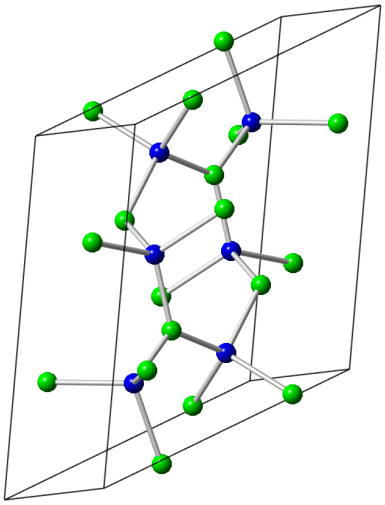

Figure 1. Representative alpha- and beta-Si_3N_4 structures, with silicon atoms shown in blue and nitrogen atoms shown in green; a) single unit cell of alpha-Si_3N_4; b) single unit cell of beta-Si_3N_4.

Amorphous Si_3N_4 models were generated by randomly generating positions for a stoichiometric ratio of Si and N atoms in sufficient number to produce a density of 3.1 g/cm^3 for a model having a total number of 14,336 atoms. After random generation of positions, a brief optimization of these positions is performed using the desired potential. The model is then heated from a temperature of 0 K to an annealing temperature of 5000 K at a rate of 10 K / ps. The model is held at this annealing temperature for 500 ps, then cooled to 300 K at a rate of 10 K / ps. This

procedure was followed using both Tersoff potential with 001 parameters as well as the SG potential, with the resulting models labeled amorphous 001 models and amorphous SG models, respectively.

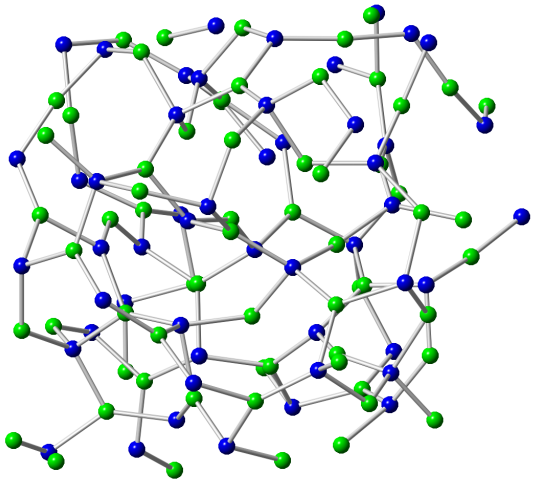

Figure 2. Representative bulk structure of amorphous Si_3N_4 models, with silicon atoms shown in blue and nitrogen atoms shown in green.

2.2. SiCN Model Generation

SiCN models were modeled as stoichiometric mixtures of Si_3N_4 and SiC with an overall composition in the glass phase of Si_4CN_4 = Si_3N_4:SiC, or $SiC_{1/4}N$, and varying amounts of excess or "free" carbon atoms. To the initial glass composition comprised of roughly 55,000 atoms, enough C atoms are added to given models to attain ratios of C_{free}:Si of 0, 0.25, 0.5, and 1. A model with glass composition Si_4CN_4 and a corresponding C_{free}:Si ratio of 1 has the composition Si_4CN_4□1C_{free} = $Si_4C_2N_4$. Models were generated such that the density of all generated models equaled 2.8 g/cm^3.

Each SiCN model obtained in this way is created by randomly generating positions for Si, C, and N atoms followed by a brief optimization. The models are then heated to a maximum temperature, called the annealing temperature, at a rate

of 0.1 K / ps. These annealing temperatures are 1000 K, 2000 K, 3000 K, 4000 K, 5000 K, 6000 K , and 7000 K. Upon reaching the desired annealing temperatures, the models are immediately cooled to 300 K at a rate of 1 K / ps.

With varying annealing temperatures, we see the formation of extended networks of "free carbon" atoms in the glass bulk. At 3000 K to 5000 K annealing temperature, the carbon atoms arrange into long, networked sheet-like extensions composed of six-membered carbon rings.

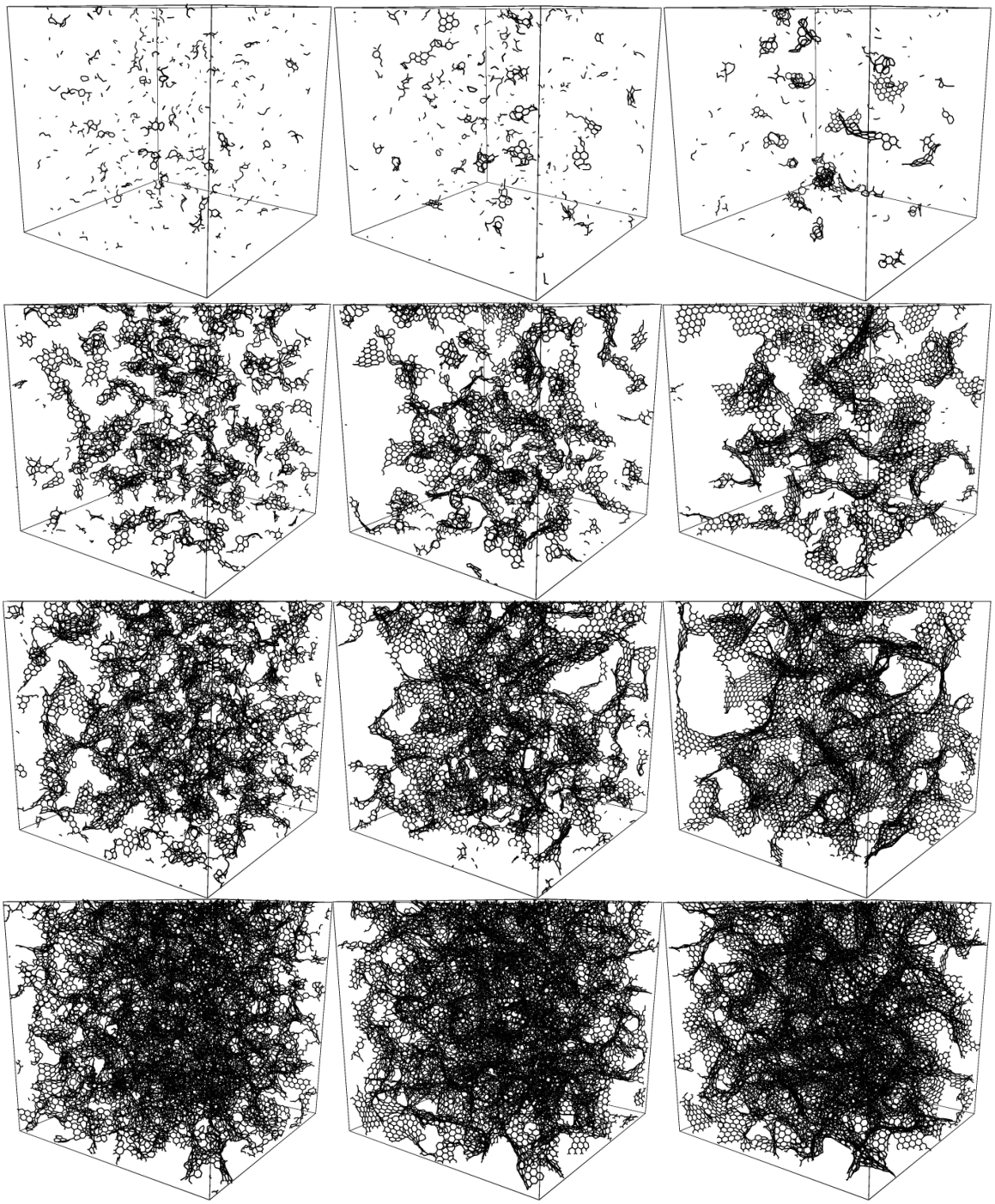

Figure 3. Amorphous SiCN models with varying carbon content and annealing temperatures; only carbon atoms shown. Rows from top to bottom: free carbon : silicon ratios 0, 0.25. 0.5, 1. Columns from left to right: maximum annealing temperatures 3000 K, 4000 K, 5000 K.

In models containing no free carbon, carbon agglomerates are localized and do not connect to one another, though increased annealing temperature drives increased carbon segregation from the bulk in carbon atoms close to one another. With a free carbon : silicon ratio of 0.25 and beyond, carbon agglomerates exhibit greater connectivity throughout the bulk, with fewer isolated agglomerates seen at an annealing temperature of 3000 K. At this carbon ratio, nearly all carbon has segregated into a single networked extension throughout the model.

2.3. Elastic Property Calculations

We use LAMMPS to compute the elastic constants c_{ij} of each obtained model using dynamic simulations at temperatures from 10 K to 2000 K; specifically, determination temparatures are 10, 200, 300, 400, 600, 800, 1000, 1200, 1400, 1600, 1800, and 2000 K. For each model, a total of 13 simulations are performed to obtain elastic constants: one for the initial state of the model plus six positive and six negative deformations along combinations of the crystal axes.

Each simulation consists of 1.0 ps of equilibration followed by sampling of the stress tensor during an 0.3 ps period. The results of the positive and negative deformations are then averaged. We then apply the Voigt-Reuss-Hill approximation to the obtained elastic constants to yield values for bulk modulus B0, Shear modulus G, and Young's Modulus E.

Each computation of elastic constants for a given model composition and determination temperature is done in triplicate, using different seeds for the random number generator employed in velocity calculation. This produces three

sets of results for each combination of model composition and determination temperature, which are then averaged to obtain reported values.

For crystalline models, the magnitude of model deformation is 2% of the lattice vector, while for amorphous models, the magnitude of this deformation is 4% of this lattice vector. These particular values were found to minimize variance of reported values between repeated calculations under the same conditions, but using different numerical seeds for random number generation.

3. Results and Discussion

3.1. Silicon Nitride Structural Data

Investigation begins with brief optimization of crystalline Si_3N_4 using the various empirical potentials under study: Tersoff (with parametrizations 001 and BM), MG2, and SG. In LAMMPS, models are optimized using the selected empirical potential and associated parameters by allowing the simulation box to relax according to parametrized interactions against an external pressure of 0 bar.

The cell parameters and densities of the models prior to optimization are provided in Table 1.

Table 1. Cell parameters and densities for crystalline silicon nitride models prior to optimization.

	a (A)	b (A)	c (A)	Density (g/cm^3)
a-Si_3N_4	54.3	53.7	56.2	3.2
b-Si_3N_4	53.5	52.9	58.4	3.2

The cell parameters and densities after optimization are provided in Table 2.

Table 2. Cell parameters and densities for crystalline silicon nitride models after optimization using various empirical potentials.

Tersoff 001	a (A)	b (A)	c (A)	Density (g/cm^3)
a-Si_3N_4	54.7	54.1	56.6	3.1
b-Si_3N_4	53.5	53.0	58.5	3.1
Tersoff BM	a (A)	b (A)	c (A)	Density (g/cm^3)
a-Si_3N_4	53.5	53.0	55.4	3.3
b-Si_3N_4	52.6	52.1	57.4	3.3
SG	a (A)	b (A)	c (A)	Density (g/cm^3)
a-Si_3N_4	53.1	52.5	54.9	3.4
b-Si_3N_4	51.9	51.4	56.7	3.5
MG2	a (A)	b (A)	c (A)	Density (g/cm^3)
a-Si_3N_4	54.3	53.7	56.2	3.2
b-Si_3N_4	53.3	52.7	58.2	3.2

We see that the two Tersoff parametrizations have opposite effects on Si_3N_4 model structure. 001 parameter set has the effect of expanding the simulation box slightly, resulting in a slightly decreased material density. The BM parameter set, however, contracts the simulation box slightly, resulting in a slightly increased material density.

The SG potential contracts all lattice parameters for simulation boxes of both alpha- and beta-Si_3N_4, though it does so more strongly for beta-Si_3N_4. This has the result of increasing material density in both cases.

The MG2 potential has a negligible effect on lattice parameters for a-Si_3N_4. However, the same potential slightly contracts all lattice parameters for b-Si_3N_4, though this has a negligible effect on material density.

3.2. Obtained Elastic Constants and Moduli of Crystalline Silicon Nitride

Elastic constants of crystalline alpha-Si_3N_4 models were determined using both parametrizations of Tersoff potential as well as with SG and MG2 potentials. The results are summarized in Table 3.

Table 3. Elastic constants of crystalline alpha-Si_3N_4 models obtained at 300 K using various empirical potentials. All constants are reported in units of GPa.

	Tersoff 001	Tersoff BM	SG	MG2	Expt. [21]
C_{11}	359.2	336.1	939.6	336.7	433.3
C_{33}	398.9	386.4	950.4	356.3	574.3
C_{12}	172.4	105.1	305.6	186	195.8
C_{13}	165.5	106.3	280.4	184	127.5
C_{44}	77.7	112.6	302	67.5	108.2
C_{66}	98.7	130.7	317.1	73.9	119.4
C_{46}	-2.5	-14.7	-20.6	-9.5	0

While the two Tersoff parametrizations and the MG2 potential roughly agree, the SG potential produces much larger values for all constants, between 200% and 300% of the values reported by the other potentials.. The MG2 potential reports constants that are are generally lower than either Tersoff parametrization for diagonal elements, but higher for C_{12} and C_{13}. Compared against the Tersoff 001 results, the MG2 potential reports values roughly 10% lower for diagonal elements and roughly 10% higher for C_{12} and C_{13}. Compared against the Tersoff BM results, the MG2 reports a value for C_{11} that agrees with Tersoff BM, but reports a nearly 10% lower value for C_{33} and a nearly 40% lower value for C_{44} and C_{66}, while reporting values for C_{12} and C_{13} that are roughly 75% higher. Between the two Tersoff

parametrizations, 001 parameters report higher values than those reported by BM parameters for all constants but C_{44}. The 001 parameters report C_{11} and C_{33} roughly 5% higher than values reported by BM parameters, while C_{12} and C_{13} values for 001 parameters are roughly 60% higher than those reported by BM parameters, and the C_{44} and C_{66} values reported by 001 parameters are roughly 30% lower than the value reported by BM parameters.

C_{11} and C_{33} are expected to be significantly different for the alpha-Si_3N_4 single crystal. All potentials report different values for C_{11} and C_{33}, but the extent of this difference is smaller for SG and MG2 potentials than either of the two Tersoff parametrizations, with the SG and MG2 potentials reporting differences between C_{11} and C_{33} of 5% or less, while both Tersoff parametrizations report differences of roughly 10%. All of these fall short of the roughly 3:4 ratio expected between C_{11} and C_{33}. C_{12} and C_{13} are also expected to be significantly different, and both Tersoff parametrizations as well as the MG2 potential present only a difference of 5% or less, while the SG potential reports a difference of nearly 10% between the two constants. Again, these differences fall short of the expected difference, which represents a roughly 3:2 ratio between the values of C_{12} and C_{13}. The reduced extent of difference between these pairs of elastic constants is attributable to the brief structure optimization prior to determination of elastic constants, as in minimizing the total energy of the structure according to a given parameter set, atomic positions will adjust slightly, thus causing a deviation from the structure according to experimentally-determined positions of atoms in the crystal lattice.

With respect to experimentally-obtained literature values, the Tersoff potential parametrizations and the MG2 potential fall short of reproducing C_{11} and C_{33} accurately, while the SG potential more than doubles the value of C_{11} and nearly doubles the value of C_{33}. The MG2 potential reports a value for C_{12} which is within 5% of the experimentally determined value, while the Tersoff 001 parametrization under-reports this value by roughly 10%, and the Tersoff BM parametrization under-reports the value by roughly 40%. The SG potential presents a C_{12} value which is roughly 50% more than the experimental value. The experimental value for C_{13} is most closely approached by the Tersoff BM parametrization, which under-reports the value by roughly 15%, with Tersoff 001, SG, and MG2 over-reporting by roughly 30%, 120%, and 45% respectively. C_{44} and C_{66} are most closely approached by the Tersoff BM parametrization, with reported values being within 5% and 10% of the experimental value respectively. The Tersoff 001 parametrization under-reports C_{44} by roughly 30% and C_{66} by roughly 20%. The SG potential over-reports both values by more than double, while the MG2 potential under-reports both values by roughly 35%.

Element C_{46} is expected to be zero, within reasonable error. It is included here as a measure of variance from expectation for each potential. Tersoff 001 most closely approaches this result, followed by the MG2 potential, then by Tersoff BM, with the SG potential presenting the most variance from the expected value of C_{46}.

Elastic moduli were determined using these same potentials across a temperature range of 10 K to 2000 K. The results are summarized in Figure 4.

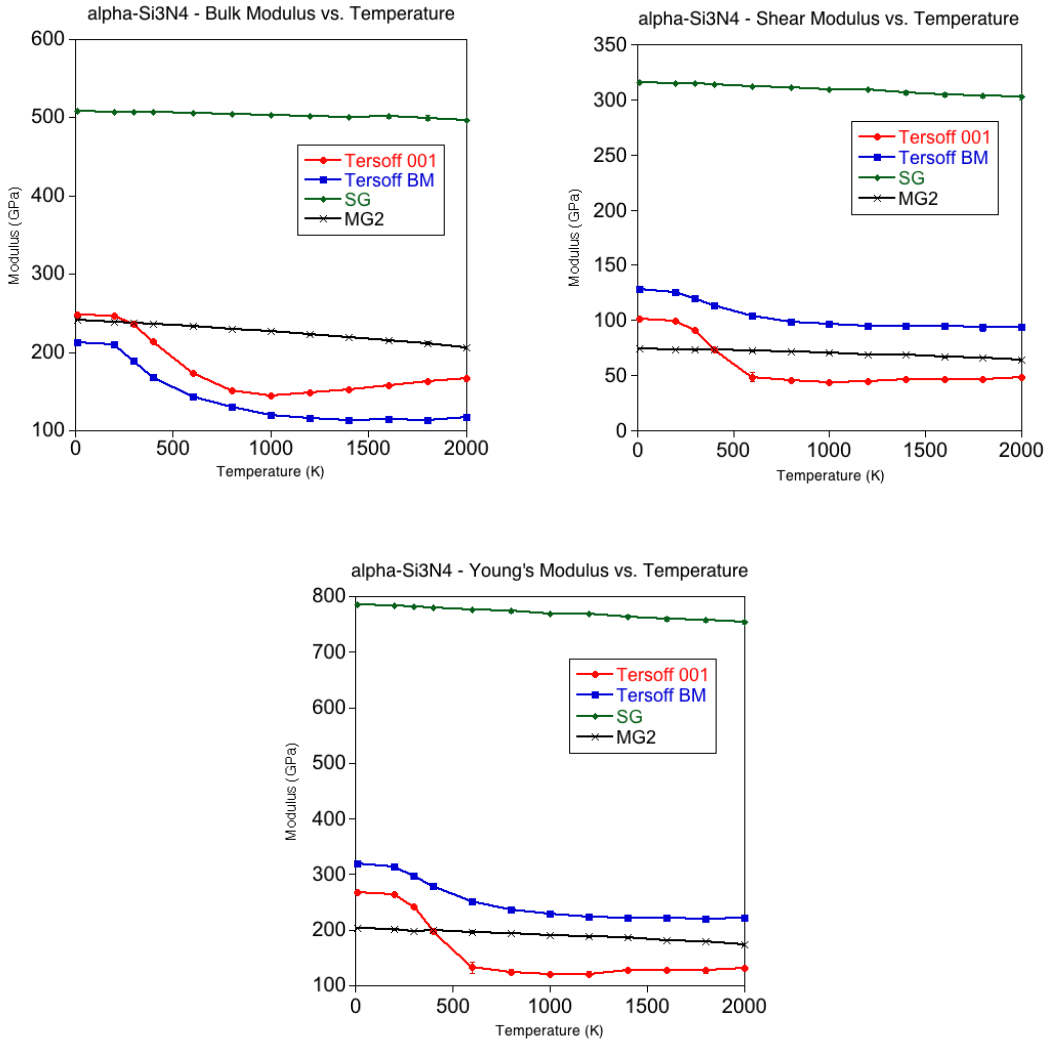

Figure 4. Obtained elastic moduli vs. calculation temperature for alpha- Si_3N_4 crystalline models using various empirical potentials.

In all cases, there is a general trend of modulus value decreasing with increasing temperature at which elastic moduli were determined, which is consistent with observations in literature [22]. Consistent with what is seen in the elastic constants at 300 K, the SG potential reports values for moduli between 200-300% of those reported by the other three potential treatments. Also of note, the SG and MG2 results show a nearly linear decrease in modulus value with increasing temperature.

However, both parametrizations of Tersoff potential present a higher slope of decrease from 10 K to 600 K for all moduli, before the nature of the trend changes. The effect is more pronounced for Tersoff 001 results than for Tersoff BM, as moduli reported by 001 drop roughly 50% in value from the 10 K measurement to the 600 K measurement, while moduli reported by BM drop by roughly 25%. For shear and Young's moduli reported by both potentials, the values of the moduli become roughly constant or slightly increase with further increases in temperature. This behavior is seen as well in the BM parametrization of Tersoff treatment for bulk modulus, but the 001 parametrization shows a significantly increasing trend for bulk modulus from 1000 K to 2000 K, increasing in value by roughly 50%. Also of note, it is seen that for bulk modulus, BM Tersoff parametrization presents a lower value for bulk modulus throughout the temperature range than the 001 Tersoff parametrization, but the opposite is seen for shear and Young's moduli.

With respect to previously obtained experimental results [23], the elastic moduli of single-crystal alpha-Si_3N_4 have been well-studied, and reported values of moduli at 300 K can be directly compared. This comparison is summarized in Table 4.

Table 4. Calculated values and literature values for alpha-Si_3N_4 elastic moduli.

	B (GPa)	G (GPa)	E (GPa)
Tersoff 001	236	91	242
Tersoff BM	189	120	297
SG	507	314	781
MG2	237	73	199
Expt. [23]	248	144	362

Against these values, the bulk modulus is most closely reproduced by the Tersoff 001 parameters and the MG2 potential. This is expected for Tersoff 001 parameters, as the bulk modulus of Si_3N_4 was one of the targets in the parameter fitting procedure [14] The shear and Young's moduli are most closely approached by the Tersoff BM parameters, though the Young's modulus is not particularly accurately reported by any potential. This suggests that choice of potential and parameter set may vary depending on the desired calculated elastic modulus. The SG potentialis more than double the experimental value for all three moduli, and thus does not seem suited to elastic property determination.

3.3. Obtained Elastic Constants and Moduli of Tersoff-Generated Amorphous Silicon Nitride

Elastic constants of Tersoff 001-generated amorphous Si_3N_4 models were determined using both parametrizations of Tersoff potential as well as with SG and MG2 potentials. The results are summarized in Table 5.

Table 5. Elastic constants of Tersoff 001-generated amorphous Si_3N_4 models calculated by various empirical potentials. All constants are reported in units of GPa.

	Tersoff 001	Tersoff BM	SG	MG2
C_{11}	305.0	274.3	404.0	136.4
C_{33}	303.5	273.8	424.5	138.7
C_{12}	132.5	82.2	164.7	62.7
C_{13}	132.2	82.4	155.0	60.1
C_{44}	90.9	96.7	126.5	40.6
C_{66}	90.9	98.2	124.5	40.1
C_{46}	-0.3	0.7	1.2	1.2

The SG potential again produces the largest values for all reported constants, though in this case the increase is on the order of 25-33% against the Tersoff results, rather than 200% or more. In this case, MG2 potential reports lower values for all constants than either Tersoff parametrization. All values reported by MG2 are consistently about 55% lower than the corresponding values reported by the Tersoff 001 parametrization. However, the difference between the MG2 and Tersoff BM parametrization results are variable; the reported MG2 values for C_{11} and C_{33} are roughly 50% lower than those reported by Tersoff BM, while the MG2 value for C_{44} is nearly 60% lower than the Tersoff BM value, and MG2 values for C_{12} and C_{13} represent only a 25% decrease against the Tersoff BM values. Between the two Tersoff parametrizations, it is again the case that 001 parameters report higher values than those reported by BM parameters for all constants except for C_{44}. Elements C_{11} and C_{33} are reported roughly 10% higher by Tersoff 001 parameters than by Tersoff BM parameters, while elements C_{12} and C_{13} are reported roughly 60% higher by 001 parameters than those reported by BM parameters, and 001 parameters report a C_{44} value roughly 5% lower than the value reported by BM parameters.

For amorphous Si_3N_4, which is expected to exhibit isotropic elastic behavior, C_{11} and C_{33} are expected to be equal. All potentials report C_{11} and C_{33} values which agree to within 5%, as expected for this pair of elements. The two Tersoff parametrizations perform the best in this regard, with agreement between C_{11} and C_{33} within 1% of values. The Tersoff parametrizations perform similarly well with respect to constants C_{12} and C_{13}, which again agree to within 1%, and the MG2

potential reports agreement between these constants within 5%. The SG potential, however, reports a 6% difference between constants C_{12} and C_{13}.

Again using element C_{46} as an example of an element expected to be zero, all potentials report similar results which are closer to the expected value than is seen in calculations performed on crystalline Si_3N_4 models.

Elastic moduli were determined using these same potentials across a temperature range of 10 K to 2000 K. The results are summarized in Figure 5.

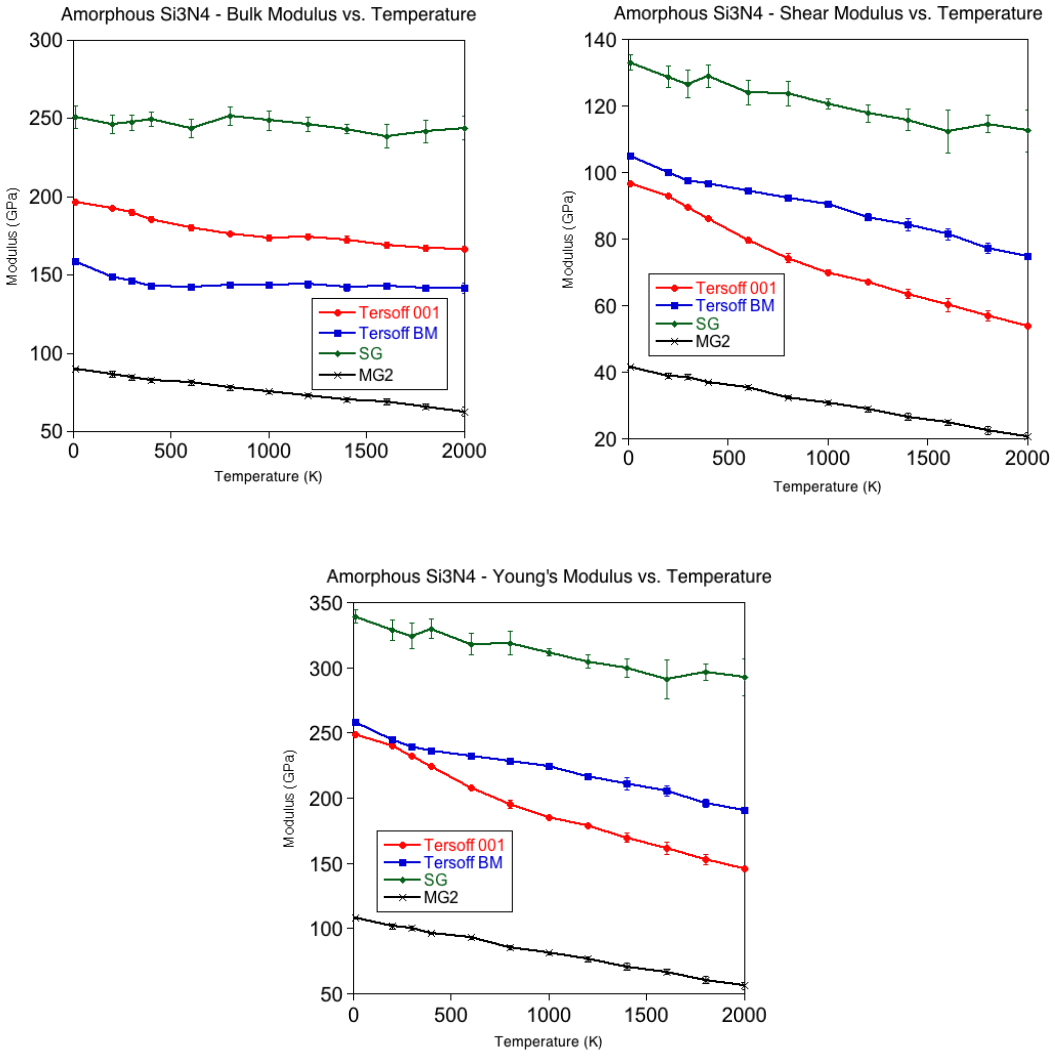

Figure 5. Obtained elastic moduli vs. calculation temperature for Tersoff 001-generated amorphous Si_3N_4 models using Tersoff 001 and BM parameter sets, SG potential, and MG2 potential.

Once more, there is a general trend of decreasing values of reported elastic moduli with increasing testing temperature, as reported in experimental literature [22]. As seen with the alpha-Si_3N_4 crystal, moduli reported using the SG potential are again much higher than those seen with all other potentials, though only on the order of a 25-33% increase against the next-highest reported values instead of the 200% or more increase seen for the crystalline model. Moduli reported by the MG2 potential

are considerably lower than all other potentials, presenting values roughly 40% of the average of Tersoff values at any given temperature. Between the two Tersoff parametrizations, we see that the 001 parameter set reports a higher bulk modulus than that reported by BM parameters throughout the temperature range, though the difference between the two decreases slightly as testing temperature increases, with 001 parameters reporting a value 25% higher than BM parameters at 10 K but a value only 20% higher at 2000 K. Conversely, the 001 parameters report lower shear and Young's moduli than those reported by BM parameters. This difference is slight at lower temperatures, but increases over the temperature range such that at 2000 K, 001 parameters report values which are roughly 30% lower than those reported by BM parameters.

Experimentally reported values of Young's modulus in amorphous Si_3N_4 vary according to determination method, but present a range from 180 – 290 GPa at room temperature [24,25]. Compared against these results, both Tersoff parameter sets perform well, reporting values from 225 – 240 GPa. In contrast, the MG2 potential presents a result close to half of the lower bound of reported experimentally-determined values, while the SG potential presents a result nearly 50 GPa above the upper bound. It thus appears that neither the SG nor the MG2 model is suitable for elastic properties determination on amorphous Si_3N_4 models generated by a melt-quench approach employing the Tersoff 001 parameter set.

3.3. Obtained Elastic Constants and Moduli of SG-Generated Amorphous Silicon Nitride

Elastic constants of SG potential-generated amorphous Si_3N_4 models were determined using both parametrizations of Tersoff potential as well as with SG and MG2 potentials. The results are summarized in Table 6.

Table 6. Elastic constants of SG-generated amorphous Si_3N_4 models calculated by various empirical potentials. All constants are reported in units of GPa.

	Tersoff 001	Tersoff BM	SG	MG2
C_{11}	305.4	276.9	723.4	232.8
C_{33}	304.3	277.5	725.1	231.3
C_{12}	134.5	83.2	261.8	116.8
C_{13}	135.0	84.5	260.8	117.1
C_{44}	90.3	96.6	237.0	58.7
C_{66}	92.8	100.2	235.0	59.4
C_{46}	-0.1	0.1	-0.5	0.4

Here, the SG potential reports values for elastic constants which are 200% or more of the values reported by the Tersoff treatments, as seen with the crystalline alpha- Si_3N_4 model. These reported constants are much larger than those reported for SG treatment of Tersoff 001-generated amorphous Si_3N_4 models, again closer to the very high values reported for the alpha- Si_3N_4 crystal. In light of these results, it may be the case that amorphous models generated by Tersoff 001 parameters present atomic positions which are in local energy minima when the model is processed using the SG potential, thus precluding any significant movement of atoms during optimization with the SG potential prior to elastic constant determination. The MG2 potential reported constants are lower than those

reported by the Tersoff 001 parametrization across the board, with C_{11} and C_{33} values for the MG2 potential being roughly 30% lower than those reported by Tersoff 001, while C_{12} and C_{13} values are 15% lower than Tersoff 001 values, and the reported C_{44} value is 55% lower than the Tersoff 001 value. Comparing against the values reported by the Tersoff BM parametrization, the MG2 potential presents values for C_{11} and C_{33} which are roughly 20% lower than those given by Tersoff BM, while values for C_{12} and C_{13} are 40% higher, and the reported C_{44} value is roughly 40% lower . Between the two Tersoff parametrizations, Tersoff 001 parameters again report higher values for all constants except for C_{44}. The 001 parameters report values for C_{11} and C_{33} which are roughly 10% higher than those reported by BM parameters, while C_{12} and C_{13} values are roughly 60% higher, and the C_{44} value is roughly 5% lower.

For all potentials, values for C_{11} and C_{33} agree to within 1%, as expected. Similarly, values for C_{12} and C_{13} agree to within 1% for all potentials as well. The better performance of the SG potential in this regard as compared to the SG treatment of Tersoff 001-generated amorphous models is likely attributable to the fact that these amorphous models were generated using the SG potential. The observation that both Tersoff parametrizations perform well with respect to agreement between constants that are expected to have the same value, regardless of the original method of generation for the amorphous models, are an indication that the Tersoff treatment outperforms the SG treatment in determination of elastic properties.

Element C_{46} values are very close to the expected value of zero for all potentials, and are observed to be closer to this expected value than is seen in elastic constant calculations on Tersoff 001-generated amorphous Si_3N_4 models.

Elastic moduli were determined using these same potentials across a temperature range of 10 K to 2000 K. The results are summarized in Figure 6.

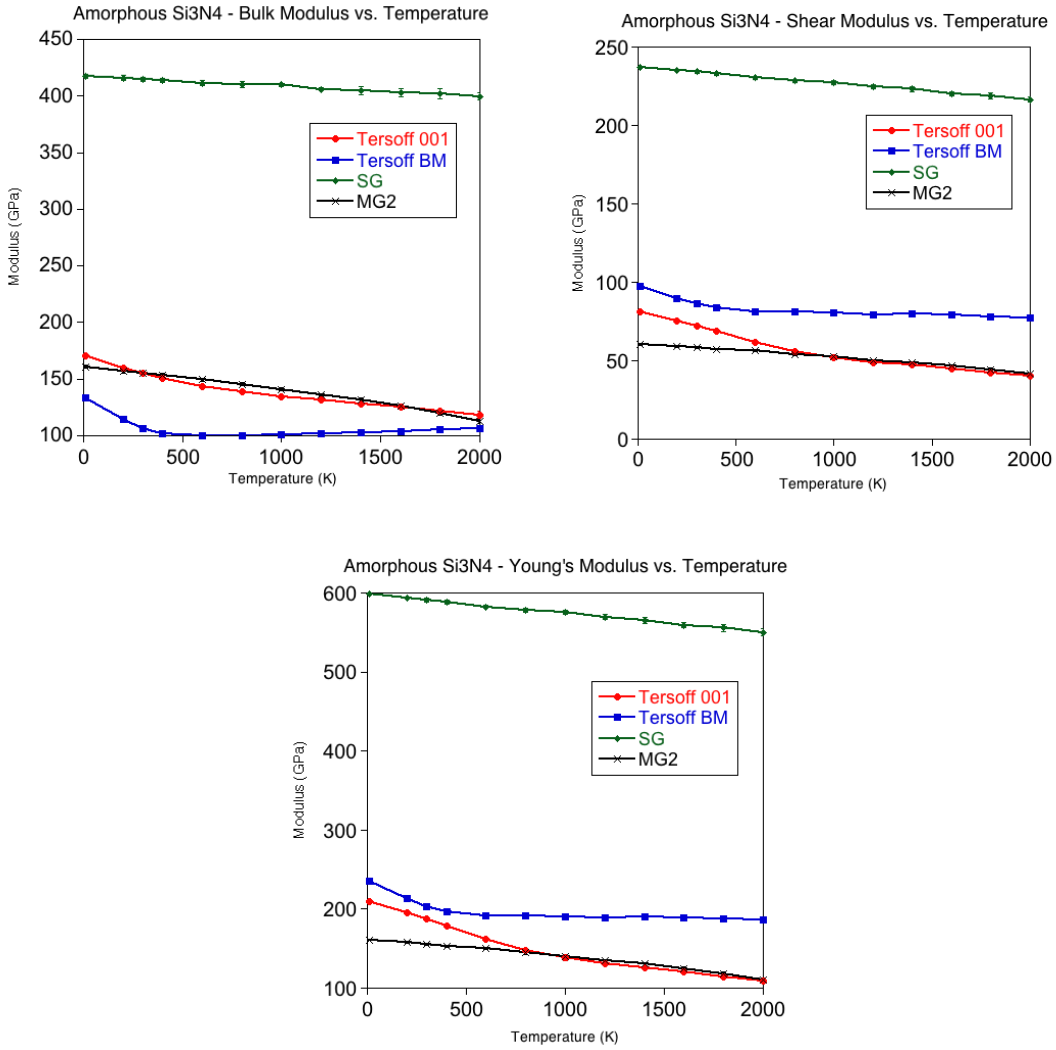

Figure 6. Obtained elastic moduli vs. calculation temperature for SG-generated amorphous Si_3N_4 models using Tersoff 001 and BM parameter sets, SG potential, and MG2 potential.

Once again, the general trend of decreasing values of reported moduli with increasing testing temperature is presented, as reported in literature [22]. As seen with reported elastic constants at 300 K, that SG reported moduli are again 200% or more of the values reported by the Tersoff and MG2 treatments. All Tersoff 001 moduli decrease throughout the temperature range, though slightly more significantly from 10 K to 1000 K, where values decrease by roughly 25% from the value at 10 K, than from 1000 K to 2000 K, where values decrease by only an additional 20% from the starting point of the 10 K measurement. In contrast, Tersoff BM moduli decrease roughly 20% from 10 K to 600 K, but shear and Young's moduli remain fairly constant thereafter up to 2000 K, while bulk modulus increases slightly over this range. The MG2 potential reports a bulk modulus which is very similar to that of Tersoff 001 bulk modulus throughout the entire temperature range, and shear and Young's moduli which are very similar in the temperature range from 1000 K to 2000 K. As with Tersoff 001-generated amorphous models, the Tersoff 001 parametrization reports higher values for bulk modulus than does the Tersoff BM parametrization, with values reported by 001 being roughly 25% higher at 10 K, though this difference decreases significantly over the temperature range such that 001 values are only roughly 10% higher at 2000 K. Conversely, the 001 parameters again present lower values for shear and Young's moduli than BM parameters at all testing temperatures, with 001 parameters being roughly 10% lower than those reported by BM parameters at lower temperatures, but the difference increasing over the temperature range such that 001 values are roughly 30% lower than BM values at 2000 K.

As noted previously, experimentally determined values for Young's modulus present a range from 180 – 290 GPa at room temperature [24,25]. Compared against these results, the Tersoff 001 parameter set presents a value at 300 K which is within 1 GPa of the lower bound. The Tersoff BM parameter set performs slightly better than this, presenting a value near 200 GPa at 300 K, though this is still at the low end of the experimentally-determined range. As seen with Tersoff 001-generated amorphous models, the MG2 potential presents a value which is short of this lower bound, though here to a lesser degree than seen with the 001-generated models, being only roughly 20 GPa short of the experimental range rather than only half of the lower bound. The SG potential again fails to approach experiment, presenting a value for Young's modulus at 300 K which is roughly double that of the upper bound of the experimentally reported range.

3.4 Obtained Elastic Moduli of Amorphous Silicon Carbonitride

As shown in Figure 3 above, the carbon morphology of SiCN models is highly dependent on the amount of carbon contained in the model as well as the maximum annealing temperature to which the model was heated during generation. With increasing carbon content or increased maximum annealing temperature, large extensions of segregated carbon are formed.

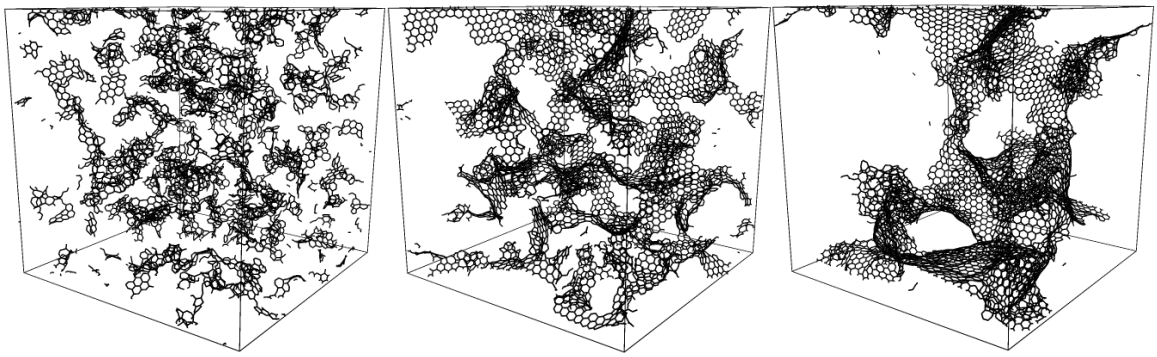

Figure 7. Amorphous SiCN models with a C_{free}:Si ratio of 0.25:1, heated to varying annealing temperatures; only carbon atoms shown. From left to right: maximum annealing temperatures 3000 K, 5000 K, 7000 K.

As seen in the above figure, at maximum annealing temperatures below 5000 K, while carbon atoms begin to bond and form segregated associations, these associations are largely isolated throughout the bulk. At a maximum annealing temperature of 5000 K, the carbon structure consists of a continuous network of graphene-like carbon arrangements distributed roughly evenly throughout the bulk. At maximum annealing temperatures above 5000 K, the carbon structure begins to concentrate at certain locations in the bulk, leaving large volumes consisting only of Si_3N_4 glass.

Elastic moduli of amorphous SiCN models were determined across a temperature range of 10 K to 2000 K using Tersoff 001 and BM parametrizations. The results for the amorphous SiCN model with a maximum annealing temperature of 5000 K are summarized in Figure 8.

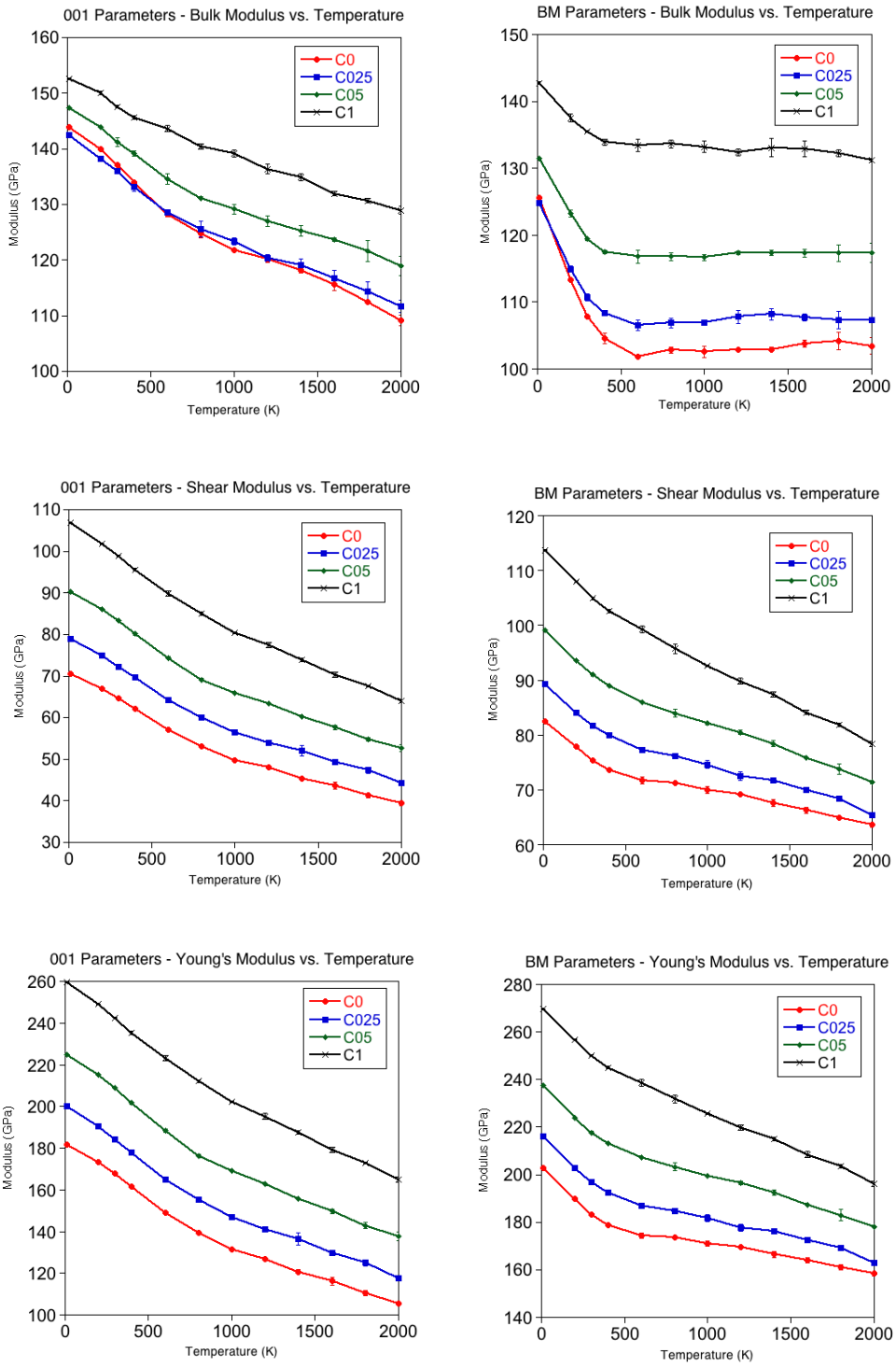

Figure 8. Obtained elastic moduli vs. calculation temperature for amorphous SiCN models using Tersoff 001 and BM parameter sets. C_{free}:Si ratios of 0, 0.25, 0.5, and 1 represented.

With both parameter sets, there is a general trend that greater amounts of free carbon in the model have the effect of increasing the value of reported moduli. Investigations in the literature are divided on this, as some sources employing standard molecular dynamics simulations to investigate elastic properties of SiCN materials report the trend of increasing moduli with increasing carbon content [15, 16] while work employing density-functional molecular dynamics simulations for investigation report the opposite trend, with modulus value decreasing as carbon content increases from a minimum of 0% carbon content to 75% carbon content[17], though this density functional work reports an increase in Young's modulus from 5% carbon content up to 10% carbon content, corresponding to the range covered in this work by silicon to excess carbon ratios 1:0.25 and 1:0.5. At lower temperatures, the bulk modulus of models with no free carbon is reported as slightly higher than that of models with a silicon to excess carbon ratio of 1:0.25. The temperature range at which this occurs is from 10 K to 400 K for 001 parameters, but only up to 200 K for BM parameters. As observed for Si_3N_4 models, bulk modulus is generally reported higher by 001 parameters than by BM parameters, though the difference between the reported values decreases with both increasing testing temperature and with increased carbon content. At a fixed testing temperature of 10 K, the bulk modulus value for models with no free carbon is reported as roughly 15% higher by the 001 parameters than by the BM parameters, but as carbon content increases, this difference diminishes to a roughly 5% higher value reported by the 001 parameters over the value reported by BM for models having a 1:1 ratio of silicon to excess carbon. For a fixed model composition

containing no excess carbon, the amount by which 001 parameters report a higher bulk modulus than BM parameters again decreases from roughly 15% at 10 K testing temperature to roughly 5% at 2000 K. These trends are preserved along comparison of the entire data set, such that models with a 1:1 ratio of silicon to free carbon report values that agree to within 2% at 2000 K. In contrast, and as also observed for Si_3N_4 models, shear and Young's moduli are reported lower by 001 parameters than by BM parameters, and the difference between the reported values increases with increased testing temperature but decreases with increased carbon content. At the testing temperature of 10 K for models containing no excess carbon, 001 parameters report a shear modulus roughly 15% lower and Young's modulus roughly 10% lower than values reported by BM parameters, with these differences increasing to roughly 35% and 25% respectively at a testing temperature of 2000 K. With respect to increasing carbon content, for a fixed testing temperature of 10 K, the differences of roughly 15% lower reported shear modulus and roughly 10% lower reported Young's modulus by 001 parameters against BM parameters for a model containing no excess carbon decrease to a roughly 10% lower reported shear modulus and roughly 5% lower reported Young's modulus for models having a 1:1 ratio of silicon to free carbon.

Previous work has reported that the value of moduli decreases significantly as temperature of elastic property determination increases [15], and this temperature-dependent effect on modulus value is replicated here. However, previous works have reported for models containing no excess carbon a Young's modulus near 260 GPa at 300 K testing temperature, which is shown to decrease to

180 GPa by 1500 K testing temperature. In this work, 001 parameters fail to capture either of these bounds accurately, with Young's modulus being reported near 180 GPa at 300 K testing temperature and dropping to nearly 120 GPa for a model with no excess carbon. The BM parameters perform better in this regard, reporting a Young's modulus near 205 GPa at 300 K and near 170 GPa at 1500 K. Previous computational work investigating effects of excess carbon content in SiCN [16] presents Young's modulus values for models corresponding to a silicon to excess carbon ratio of 1:1 of 280 GPa at 300 K testing temperature, decreasing over the testing temperature range to a minimum near 250 GPa at 1500 K. Here, both parameter sets more closely approach the previously reported values, with 001 parameters reporting a value near 235 GPa at 300 K with a value near 190 GPa at 1500 K, and BM parameters reporting a value near 250 GPa at 300 K with a value near 215 GPa at 1500 K.

Investigating the trends in reported moduli with respect to maximum annealing temperatures and thus carbon network formation of amorphous SiCN models with both parameter sets, the results attained for elastic moduli determination at 300 K are summarized in Figure 9.

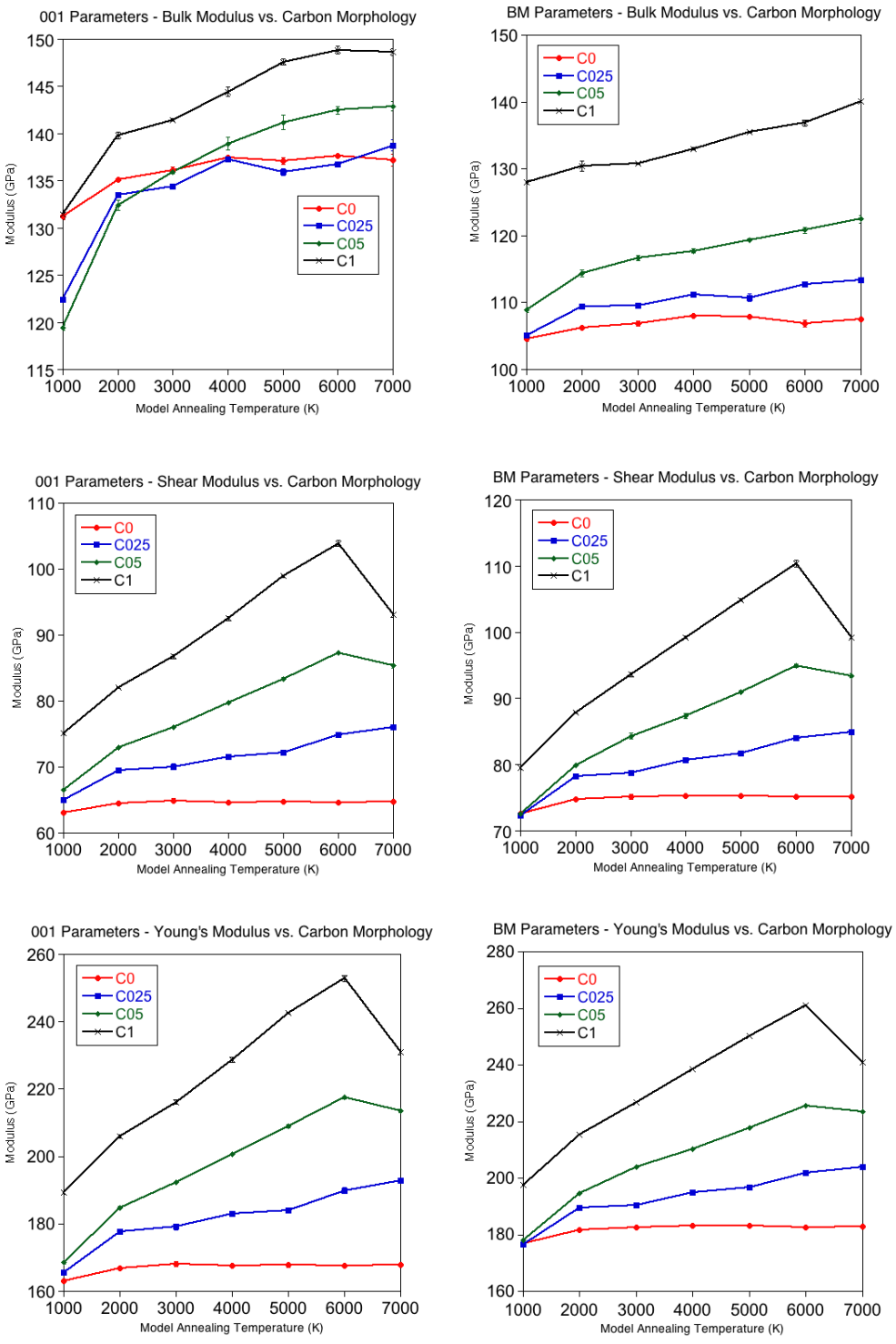

Figure 9. Obtained elastic moduli vs. carbon morphology for amorphous SiCN models using Tersoff 001 and BM parameter sets. C_{free}:Si ratios of 0, 0.25, 0.5, and 1 represented. Here, model annealing temperature is used to provide a measure for overall carbon morphology as demonstrated in previous figures.

For all moduli reported by BM parameters, and for shear and Young's moduli reported by 001 parameters, there is a trend of increasing modulus value with increasing free carbon content across all annealing temperatures. However, bulk modulus reported by 001 parameters does not preserve this trend. While the highest reported values for bulk modulus are attained by the model with a silicon to excess carbon ratio of 1:1, at maximum annealing temperatures below 3000 K, the bulk modulus decreases with increasing carbon content from silicon to excess carbon ratios of 1:0 up to 1:0.5. Beyond maximum annealing temperatures of 3000 K, bulk modulus for models with a silicon to excess carbon ratio of 1:0.5 is higher than those with lower free carbon content, while models with silicon to free carbon ratios of 1:0 and 1:0.25 are similar throughout the range of maximum annealing temperatures. Once again, 001 parameters report a higher bulk modulus and lower shear and Young's moduli than do BM parameters across the maximum annealing temperature range. The difference between reported values by each parameter set remain roughly constant as maximum annealing temperature increases, with 001 parameters reporting roughly 25% higher values for bulk modulus, roughly 15% lower values for shear modulus, and roughly 5% lower values for Young's modulus than those reported by the BM parameters across all maximum annealing temperatures.

4. Conclusion

The Tersoff potential appears to be a good choice for these calculations. In contrast, while the SG potential and MG2 potential have shown in this work and in prior experimental work to be suitable for structure generation, the data here suggest that they are not suitable for elastic properties determination by the method used here. The Tersoff potential appears particularly suitable for amorphous configurations, which do not exhibit the significant sensitivity of reported values on minor shifts in structure induced by optimization with a particular empirical potential which are seen in crystalline models.

With respect to silicon nitride and the two parameter sets used for the Tersoff potential in this work, Tersoff 001 parameters more closely approach experimental values for bulk modulus, while the Tersoff BM parameters more closely approach experimental values for Shear and Young's moduli. This suggests that the BM parameters are more accurate in determining energy differences in cases where the angles between atoms are being significantly changed.

While all potentials managed to reproduce the trend of decreasing modulus value with increasing testing temperature reported in literature [22], the magnitude of decrease with increasing temperature was captured accurately only by the SG potential. Both of the Tersoff parametrizations and the MG2 potential present high values for elastic moduli at high temperature compared with available literature data. While the SG potential properly reflects the expected magnitude of decrease from low temperature to high temperature, it does not report reasonable values for elastic moduli overall. Therefore, there is a need for some parametrization of an

empirical potential which can accurately reproduce the high-temperature elastic behavior of SiN and SiCN materials.

Experimental investigation of the elastic properties of graphene reports very high values for elastic moduli, with Young's modulus reported near 1000 GPa [26,27]. In light of this, we can infer that a mixture of silicon nitride and excess carbon, where the carbon has taken on a graphene character as exhibited by the models in this work, should exhibit elastic modulus values which are higher than that of the pure Si_3N_4, though lower than that of pure graphene. This expectation is met by the calculations performed here, as modulus values increase with increased excess carbon content, as well as tending towards maximum values at annealing temperatures which yield graphene-like arrangements of the segregated excess carbon.

This increase in modulus value with increased excess carbon content is highly dependent on the particular carbon morphology found in carbon domains, as annealing temperatures too low to drive formation of an interconnected graphene structure or sufficiently high as to form large regions of SiN glass bulk without significant carbon content are associated with lower modulus values than those reported for models with well-formed graphene-like carbon domains. Further, for models having the same density and composition, it is shown here that models with isolated carbon segregations with limited interconnectivity exhibit a weaker sensitivity of increase in modulus value with increase in excess carbon content than do models with fully interconnected carbon segregations. Similarly, models with the same density and composition which have fully interconnected carbon

segregations that nonetheless segregate so significantly as to leave large regions of SiN glass bulk exhibit this same reduced sensitivity towards modulus value increase with increasing excess carbon content..

References

[1] Y. Huang, X. Duan, Y. Cui, L.J. Lauhon, K.-H. Kim, C.M. Lieber. Logic gates and computation from assembled nanowire building blocks, Science 294 (2001) 1313–1317.

[2] E. Comini, G. Faglia, G. Sberveglieri, Z. Pan, Z.L. Wang. Stable and highly sensitive gas sensors based on semiconducting oxide nanobelts, Appl. Phys. Lett. 81 (2002) 1869–1871.

[3] B.S. Bal, M. Rahaman. Orthopedic applications of silicon nitride ceramics, Acta Biomater. 8 (2012) 2889–2898.

[4] J. Han, J. Fu, R.B. Schoch. Molecular sieving using nanofilters: past, present and
future, Lab Chip 8 (2008) 23–33.

[5] R. Riedel, H.-J. Kleebe, H. Schönfelder, F. Aldinger. A covalent Micro/nano-composite resistant to high-temperature oxidation, Nature, 374 (1995), 526-528.

[6] L. An, R. Riedel, C. Konetschny, H.-J. Kleebe, R. Raj. Newtonian viscosity of amorphous silicon carbonitride at high temperature, J. Am. Ceram. Soc., 81 (1998), 1349-1352.

[7] R. Riedel, L. Ruwisch, L. An, R. Raj. Amorphous silicoboron carbonitride ceramic with very high viscosity at temperatures above 1500°C, J. Am. Ceram. Soc., 81 (1998), 3341-3344.

[8] R. Coustel, M. Haacke, V. Rouessac, J. Durand, M. Drobek, A. Julbe. An insight into the structure-property relationships of PECVD SiCxNy(O):H materials. Micropor. Mesopor. Mat., 191 (2014), 97-102.

[9] S. Peter, M. Gunther, S. Berg, A. Clausner, F. Richter. Mid-frequency PECVD of a-SiCN:H films and their structural, mechanical and electrical properties. Vacuum, 90 (2013) 155-159.

[10] D. Kumar, B.P. Swain. Investigation of structural and mechanical properties of silicon carbonitride thin films. J. Alloys Compd., 789 (2019) 295-302.

[11] S. Ma, B. Xu, G. Wu, Y. Wang, F. Ma, D. Ma, K. Xu, T. Bell. Microstructure and mechanical properties of SiCN hard films deposited by an arc enhanced magnetic sputtering hybrid system. Surf. Coat. Technol., 202 (2008) 5379-5382.

[12] N. Janakiraman, F. Aldinger. Fabrication and characterization of fully dense Si-C-N ceramics from a poly(ureamethylvinyl)silazane precursor. J. Eur. Ceram. Soc., 29 (2009), 162-173.

[13] Z.L. Sun, Y. Zhou D.C. Jia, X.M. Duan, Z.H. Yang, D. Ye, P.F. Zhang, Q. Zhang. Mechanical and thermal physical properties of amorphous SiCN(O) ceramic bulks prepared by hot-press sintering. Mater. Lett., 72 (2012), 57-59.

[14] P.M.Kroll, Ph.D thesis, Computersimulationen und Röntgennahkantenabsorptionsspektroskopie von Siliciumnitrid und Siliciumcarbidnitrid Keramiken, Technische Hochschule (Darmstadt, 1996).

[15] J. Jia, D. Zhou, J. Zhang, F. Zhang, Z. Lu, C. Pu. First-principles investigation of elastic and thermodynamic properties of SiCN under pressure. Comp. Mater. Sci., 95 (2014) 228-234.

[16] N. Liao, G. Ma, M. Zhang, W. Xue. Effects of SiC particles on mechanical properties of SiCN-based composite by atomistic simulation. Compos. Part B-Eng., 43 (2012) 1739-1742.

[17] N. Liao, W. Xue, M. Zhang. Effect of carbon content on structural and mechanical properties of SiCN by atomistic simulations. J Eur. Ceram. Soc., 32 (2012) 1275-1281.

[18] G. Lehmann, P. Hess, J.J. Wu, C.T. Wu, T.S. Wong, K.H. Chen, L.C. Chen, H.Y. Lee, M. Amkreutz, Th. Frauenheim. Structure and elastic properties of amorphous silicon carbon nitride films. Phys. Rev. B., 64 (2001) 165305.

[19] A. Dasmahapatra, P. Kroll. Modeling amorphous silicon nitride: A comparative study of empirical potentials, Comp. Mater. Sci., 148 (2018) 165-175.

[20] M. Billy, J. Labbe, A. Selvarag, G. Roult. Modifications structurales du nitrure de silicium en foncion de la temperature. Mater. Res. Bull., 18 (1983), 921-934.

[21] R. Vogelgesang, M. Grimsditch, J.S. Wallace. The elastic constants of single-crystal beta-Si_3N_4. Appl. Phys. Lett., 76 (2000), 982.

[22] I. Tomeno. High temperature elastic moduli of Si_3N_4 ceramics. Jpn. J. Appl. Phys., 20 (1981) 1751.

[23] O. Yeheskel, Y. Gefen. The effect of the alpha phase on the elastic properties of Si_3N_4. Mater. Sci. Eng., 71 (1985) 95-99.

[24] A. Khan, J. Philip, P. Hess. Young's modulus of silicon nitride used ins canning force microscope cantilevers. J. Appl. Phys., 95 (2004), 1667.

[25] M. Vila, D. Caceres, C. Prieto. Mechanical properties of sputtered silicon nitride thin films. J. Appl. Phys., 94 (2003), 7868.

[26] C. Lee, X. Wei, J.W. Kysar, J. Hone. Measurement of the elastic properties and intrinsic strength of monolayer graphene. Science, 321 (2008), 385-388.

[27] C. Lee, X. Wei, Q. Li, R. Carpick, J.W. Kysar, J. Hone. Elastic and frictional properties of graphene. Phys. Status Solidi B, 246 (2009), 2562-2567.